Migration of Trace Elements from Pyrite Tailings in Carbonate Soils

C. Dorronsoro,* F. Martin, I. Ortiz, I. García, M. Simón, E. Fernández, J. Aguilar, and J. Fernández

ABSTRACT

In the carbonate soils contaminated by a toxic spill from a pyrite mine (Aznalcóllar, southern Spain), a study was made of a thin layer (thickness = 4 mm) of polluted soil located between the pyrite tailings and the underlying soil. This layer, reddish-yellow in color due to a high Fe content, formed when sulfates (from the oxidation of sulfides) infiltrated the soil, causing acidification (to pH 5.6 as opposed to 8.0 of unaffected soil) and pollution (in Zn, Cu, As, Pb, Co, Cd, Sb, Bi, Tl, and In). The less mobile elements (As, Bi, In, Pb, Sb, and Tl) concentrated in the uppermost part of the reddish-yellow layer, with concentration decreasing downward. The more mobile elements (Co, Cd, Zn, and Cu) tended to precipitate where the pH was basic, toward the bottom of the layer or in the upper part of the underlying soil. The greatest accumulations occurred within the first 6 mm in overall soil depth, and were negligible below 15 mm. In addition, the acidity of the solution from the tailings degraded the minerals of the clay fraction of the soils, both the phyllosilicates as well as the carbonates. Also, within the reddish-yellow layer, gypsum formed autigenically, together with complex salts of sulfates of Fe, Al, Zn, Ca, and Mn, jarosite, and oxihydroxides of Fe.

As the result of a break in the retention wall of a pond containing the residues of a pyrite mine in Aznalcóllar (Seville province, southern Spain) on 25 Apr. 1998, 45×10^5 m^3 of toxic water and tailings containing high concentrations of heavy metals were spilled, affecting 45 km^2 of land within the Agrio and Guadiamar River basins. The concentration of heavy metals in the waters was minimal (measured in μg kg^{-1}; Simón et al., 1999), implying that the soil pollution was caused exclusively by the tailings, which penetrated irregularly through pores and cracks (Simón et al., 1999).

From the spill, the soils were covered by a layer of tailings (Fig. 1) of variable thickness averaging 7 cm (López-Pamo et al., 1999). When the tailings from a pyrite mine are exposed to oxygen and water, sulfides oxidize to sulfates, the pH falls markedly due to the formation of sulfuric acid, and the pollutants solubilize (Nordstrom, 1982; Förstner and Wittmann, 1983; Nordstrom and Alpers, 1999; Alastuey et al., 1999).

In the carbonate soils the penetration of the liquid phase from the tailings was strongly limited because the carbonates neutralized the acidity of the solution, the oxidation of Fe^{2+} to Fe^{3+} proceeds rapidly (Singer and Stumm, 1968), iron precipitates and the calcium and sulfate ions form gypsum (Ritsema and Groenenberg, 1993; Kashir and Yanful, 2000), precipitating most of the heavy metals and trace elements. Gypsum formation in these soils is therefore frequent both in the presence of carbonates as well as calcium from mineral alteration or from calcium adsorbed by the exchange complex (Van Breemen, 1973). Thus, the mobility of heavy metals released in these processes is related to pH and Eh, to the complex ion forms involved, and to the presence of certain soil components that favor adsorption (most commonly $CaCO_3$, clays, organic matter, and oxy-hydroxides of iron, aluminum, and manganese).

In some places in these soils, a thin layer of reddish-yellow soil (a few millimeters thick) developed immediately underneath the tailings (Fig. 1). This layer appeared a few weeks after the spill, the color being owed to abundance of Fe in the tailings (Simón et al., 1999). Presumably, this layer resulted from the impregnation of the soil by contaminating solutions from the overlying layer of tailings.

The aim of the present work is to assess, in the reddish-yellow layer of these soils (where the toxic spill exerted its most intense effects), the level of pollution, the migration of the pollutant elements, and the chemical consequences of this pollution in the soil.

MATERIALS AND METHODS

Three reddish-yellow layers, 4 mm thick each, were sampled on 20 June 1998 (57 days after the spill). Within these layers, the soil was sampled every millimeter (0–1, 1–2, 2–3, and 3–4 mm), and the underlying soils were also sampled at various depths (4–6, 13–15, 28–30, and 100–150 mm). In addition, the layer of tailings covering the reddish-yellow layers was also sampled. Furthermore, three adjacent soils unaffected by the spill (0–100 mm) were used as the background.

In each sample, the particle-size distribution was determined by the pipette method after elimination of organic matter with H_2O_2 and dispersion with sodium hexametaphosphate (Loveland and Whalley, 1991). The pH was measured potentiometrically in a 1:2.5 soil–water suspension. The $CaCO_3$ equivalent was determined by a manometric method (Williams, 1948). Total carbon was analyzed by dry combustion with a LECO (St. Joseph, MI) instrument, and the organic carbon was determined by the difference between total carbon and inorganic carbon from $CaCO_3$. The cation exchange capacity (CEC) was determined with 1 M Na-acetate at pH 8.2. Pills of soil and lithium tetraborate (0.6:5.5) were prepared and the total content in Fe was measured by X-ray fluorescence using a Philips (Eindhoven, the Netherlands) PW-1404 instrument.

Samples of the tailings and soils, very finely ground (<0.05 mm), were digested in strong acids (HNO_3 + HF + HCl). In each digested sample, 25 elements were measured by inductively coupled plasma mass spectrometry (ICP–MS) with a PerkinElmer (Wellesley, MA) SCIEX ELAN-5000A spectrometer. The accuracy of the method was corroborated by analyses (six replicates) of Standard Reference Material SRM 2711 (Simon et al., 1999). A Zeiss (Oberkogeem, Germany) 950 scanning electron microscope with a Tracor Northern 523 X-ray energy-scattering microanalyzer (scanning electron microscopy [SEM]–energy dispersive spectrometry [EDS]) (Link Isis, Oxford, UK) was used to examine the morphology and analyze the composition of certain minerals present in the first 6 mm of the soil. For X-ray diffraction, a Philips PW-1710 instrument with CuKα radiation was used.

The climate of the study area is typically Mediterranean (hot, dry summers; cold, wet winters; temperate autumns; and springs with variable rainfall). The average annual rainfall is

Departamento Edafología, Facultad de Ciencias, Universidad de Granada, 18002 Granada, Spain. Received 24 May 2001. *Corresponding author (cfdorron@goliat.ugr.es).

Published in J. Environ. Qual. 31:829–835 (2002).

Abbreviations: MI, migration index.

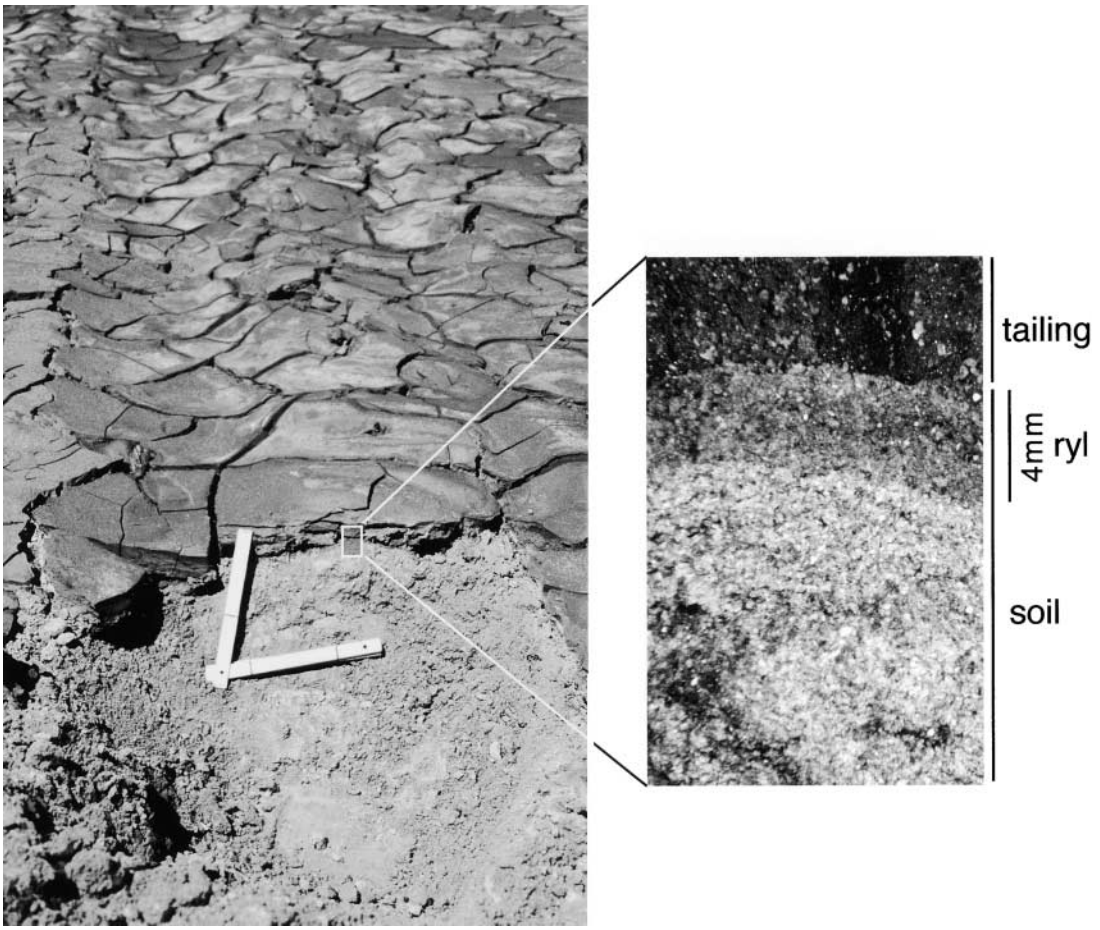

Fig. 1. Layer of tailings covering the soils as result of the toxic spill and detail of the reddish-yellow layer (ryl) at the contact point between the tailings and soil (thickness of the reddish-yellow layer was 4 mm).

630 mm, the average temperature 17.9°C, and the potential evapotranspiration 975 mm.

RESULTS AND DISCUSSION

Soil Properties and Main Components

The soils that presented reddish-yellow layers were sandy carbonate with low organic-matter content, moderate cation exchange capacities, low pH, and little iron (approximately 3%; Table 1). These layers presented the Munsell color 7.5YR6/8, while the rest of the soil had the color 10YR6/3.

The oxidation of the sulfides in the tailings caused a sulfate-rich contaminant solution (Stumm and Morgan, 1981) that on infiltration with rainwater strongly acidified the soil. The infiltration of the acidic solution decarbonated and acidified the reddish-yellow layer (the first 4 mm of the soil). The carbonate content diminished in this layer by up to 85% with respect to the underlying soil (Table 2). The iron within this layer strongly increased (Table 2), indicating a high degree of pollution. Also, from this Fe distribution, we deduce that this metal was responsible for the reddish-yellow color. The infiltration of the acidic solution led to hydrolysis of the finest mineral particles, reducing the mean clay content by roughly 62% with respect to the underlying soil. In addition, the organic-carbon content declined by 45% in the reddish-yellow layer.

The X-ray diffractograms of the underlying soil indicate a mineralogy primarily of quartz, feldspar, calcite, and, in lesser quantity, dolomite (Fig. 2). In the soil samples within the layer, abundant gypsum formed (Rit-

Table 1. Uncontaminated soils (0–100 mm). Values, mean, and standard errors (SE) of the pH, particle size, organic carbon (OC), cation exchange capacity (CEC), $CaCO_3$, and total Fe.

Soils	pH	Sand	Silt	Clay	OC	CEC	$CaCO_3$	Fe
		%				$cmol_c\ kg^{-1}$	%	
Soil A	7.8	50.8	20.5	18.5	0.69	10.3	13.6	2.32
Soil B	8.0	52.3	27.2	20.5	1.52	14.6	8.3	2.97
Soil C	8.2	57.8	24.6	17.1	0.89	9.3	18.5	1.15
					Statistical			
Mean	8.0	53.6	24.1	18.7	1.03	11.4	13.5	2.15
SE	0.1	2.1	1.9	1.0	0.25	1.6	2.9	0.53

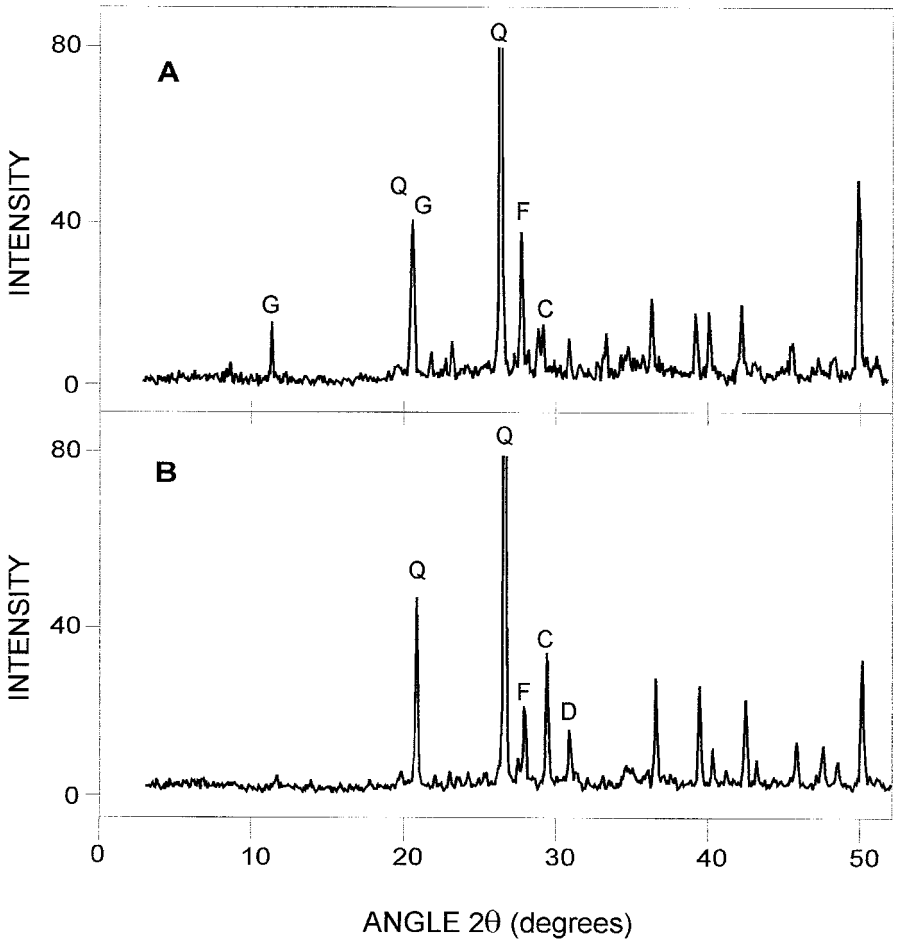

Fig. 2. X-ray diffractograms of a powder sample from soil within (*A*) and below (*B*) the reddish-yellow layer. G, gypsum; Q, quartz; F, feldspars; C, calcite.

sema and Groenenberg, 1993; Kashir and Yanful, 2000), while the peaks corresponding to carbonates strongly decreased. In no case was pyrite detected, revealing the complete lack of direct contamination by the tailings in the interior of the layer (this fact was corroborated by electron microscopy).

The oriented aggregates of the clay fraction in the samples from the soil underlying the reddish-yellow layer gave diffractograms showing illite, kaolinite, smectite, interstratified complexes of chlorite–smectite, calcite, and feldspars. In the samples from the interior of this layer, the peaks become broader and lower, indicating a generalized breakdown of minerals, both of the phyllosilicates as well as carbonates (Fig. 3). The presence and alteration of the components present in the soil (fundamentally, feldspars, micas, and clays) boosted the capacity of acid neutralization and retention of released metals. Identification of such mineral alteration is not easy, the phyllosilicates and particularly smectites apparently being the most active in neutralizing the acidity (Pons et al., 1982; Van Breemen, 1980).

Electron microscopy of the reddish-yellow layer confirmed the presence of gypsum (Miedema et al., 1974; Eswaran and Shoba, 1983) together with sulfates that had highly diverse compositions (sometimes jarosite; Wagner et al., 1982; Eswaran and Shoba, 1983) as well

Table 2. Mean values of the pH, particle size, organic carbon (OC), cation exchange capacity (CEC), $CaCO_3$, and total Fe (Fe) content at different depths in contaminated soils (values for the reddish-yellow band are listed in italic type). SE, standard error; nd, not determined.

Depth	pH		Sand		Silt		Clay		OC		CEC		$CaCO_3$		Fe	
mm		SE	%	SE	%	SE	%	SE	%	SE	$cmol_c\ kg^{-1}$	SE	%	SE	%	SE
0–1	*5.6*	*0.2*	*nd*	*nd*	*nd*	*nd*	*5.6*	*0.9*	*0.41*	*0.08*	*nd*	*nd*	*nd*	*nd*	*5.46*	*0.5*
1–2	*6.0*	*0.1*	*nd*	*nd*	*nd*	*nd*	*5.9*	*0.8*	*0.33*	*0.04*	*nd*	*nd*	*3.3*	*0.5*	*4.62*	*0.7*
2–3	*6.3*	*0.1*	*nd*	*nd*	*nd*	*nd*	*6.4*	*0.8*	*nd*	*nd*	*nd*	*nd*	*1.9*	*0.4*	*4.09*	*0.6*
3–4	*6.8*	*0.1*	*nd*	*nd*	*nd*	*nd*	*6.7*	*0.8*	*nd*	*nd*	*nd*	*nd*	*3.0*	*0.2*	*3.99*	*0.3*
4–6	7.6	0.1	nd	nd	nd	nd	11.0	0.4	0.49	0.05	nd	nd	10.5	0.9	2.70	0.2
13–15	7.9	0.1	nd	nd	nd	nd	11.4	0.5	0.50	0.03	nd	nd	12.7	1.1	2.73	0.3
28–30	8.0	0.1	nd	nd	nd	nd	11.7	0.8	0.55	0.02	nd	nd	13.1	1.0	2.76	0.3
100–150	8.0	0.1	53.2	2.2	32.1	1.6	14.7	1.4	0.60	0.07	16.2	1.5	12.8	0.6	2.89	0.2

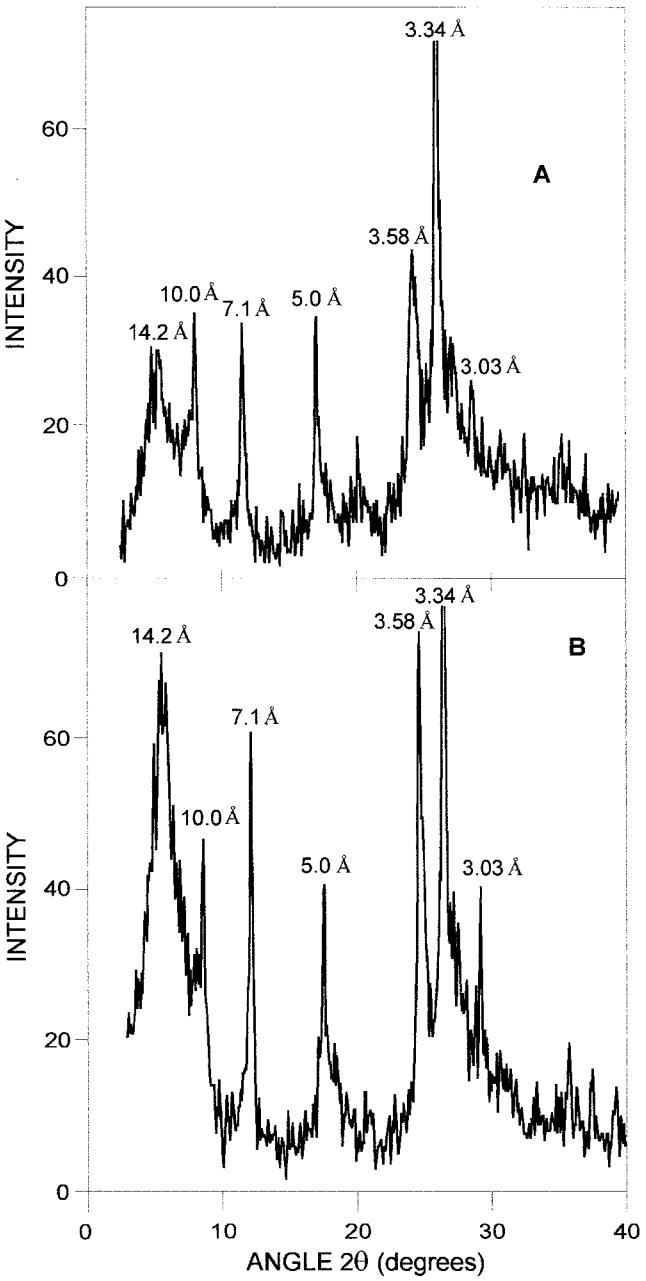

Fig. 3. X-ray diffractograms of an oriented aggregate sample from soil within (*A*) and below (*B*) the reddish-yellow layer.

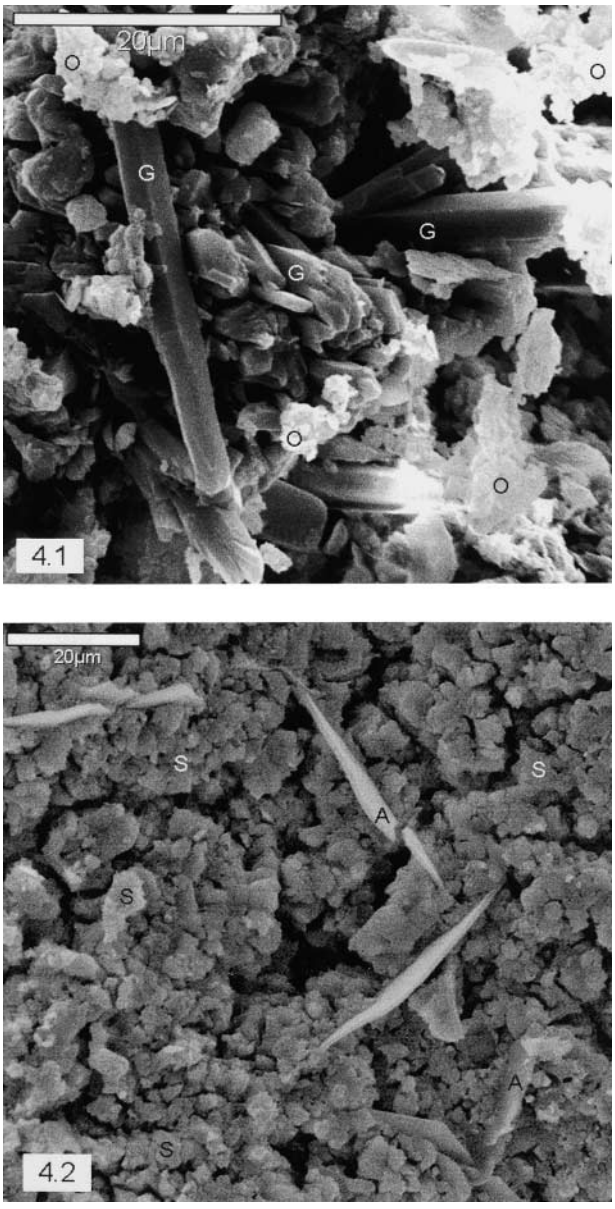

Fig. 4. Microphotography by scanning electron microscopy (SEM) of soils in the interior of the reddish-yellow layer (at 2 mm from the contact point with the tailings). Photo 4.1: (SEM–energy dispersive spectrometry [EDS]) tabular crystals of gypsum (G) in a mass of Fe oxyhydroxides (O). Photo 4.2: (SEM–EDS) acicular crystals of Al sulfate (A) in a mass of sulfates of Fe, Al, Zn, and Ca (S).

as Fe oxides and hydroxides in much lower proportions (Fig. 4). In carbonate soils affected by acid solutions the presence of iron oxyhydroxide coatings over calcite grains with substantial amounts of adsorbed Zn, Cu, and Pb have been described (Bertorino et al., 1995). Electron microscopy of these samples also revealed that the S, Fe, and Al constituted main elements, while Zn, Mn, and K were found in lesser concentrations. These results indicate that, in addition to the precipitation as gypsum, sulfates may also be adsorbed by various Fe and Al oxides and hydrous oxides, this being assumed to be the primary mechanism for SO_4^{2-} retention in a variety of soils (Parfitt and Smart, 1978; Johnson and Todd, 1983; Singh, 1984). The Fe compounds were more abundant in the upper part of the layer (0–3 mm), whereas the Al sulfates, and at times with Zn, were concentrated below (4–6 mm).

Elemental Composition

A total of 25 trace elements were analyzed (Table 2). According to the analysis of variance (ANOVA), the values of the different layers of polluted vs. nonpolluted soils (values for the same nonpolluted soils being similar to those of Simon et al. [1999], Lopez-Pamo et al. [1999], and Cabrera et al. [1999]) showed significant increases in Pb, Zn, As, Cu, Sb, Bi, Tl, Co, Cu, and In; therefore, only 10 elements were deemed pollutants.

The reddish-yellow layer showed high contents of

Table 3. Mean elemental composition and standard errors (SE). The values of Columns 0–1, 1–2, 2–3, and 3–4 represent the depth of the sample in mm and correspond to the soil within the reddish-yellow layer. The soil samples at 4–6, 13–15, 28–30, and 100–150 mm lay below this layer. T represents the sample of tailings in contact with the reddish-yellow layer and UCS the uncontaminated soil (0–100 mm).

	0–1		1–2		2–3		3–4		4–6		13–15		28–30		100–150		UCS		T	
	Mean	SE	Mean	SE	Mean	SE	Mean	SE	Mean	SE	Mean	SE	Mean	SE	Mean	SE	Mean	SE	Mean	SE
	mg kg^{-1}																			
Pb	1 482.1***	86.2	1 168.5**	146.4	779.7**	94.3	470.0**	82.2	80.0	12.5	114.7	12.4	90.0	7.8	98.3	12.3	81.6	6.1	9 507.3	1 047.3
Zn	6 939.5***	153.0	7 527.1***	419.1	10 200.0***	424.7	23 090.0***	461.8	6 178.1***	155.5	2 043.2***	73.7	673.5***	35.6	294.3**	31.9	100.4	3.0	8 063.4	426.7
As	2 233.7***	97.7	1 008.4***	73.1	620.8***	46.9	280.4**	36.4	31.4*	1.3	44.0***	1.4	28.6	1.1	31.4	1.6	25.8	1.3	4 094.1	165.5
Cu	3 387.0***	147.0	4 557.4***	456.5	7 835.0***	1 000.3	11 480.0***	989.8	131.4***	4.4	165.6***	12.5	144.7***	6.0	38.2**	2.3	25.7	0.4	2 175.8	205.6
Sb	22.9**	2.7	10.6***	1.0	7.2***	0.3	6.3***	0.4	2.8**	0.2	4.4***	0.3	3.4**	0.3	3.3**	0.2	1.9	0.1	820.1	68.8
Ba	211.4	17.8	209.2	15.1	210.0	48.6	218.6	8.7	246.4	12.7	255.0	12.6	251.3	29.1	273.5	19.7	296.3	10.7	794.3	72.8
Mn	334.2	7.4	359.8	16.2	364.0	4.5	648.3	81.2	804.8	67.1	756.7	136.3	734.2	55.1	789.3	19.6	816.3	120.5	723.8	34.2
Bi	12.7***	1.4	7.1***	0.5	4.4***	0.3	2.2***	0.2	0.5*	0.0	0.5	0.0	0.4	0.0	0.4	0.0	0.4	0.0	85.9	8.1
Tl	5.9***	0.2	4.2***	0.1	4.4***	0.4	4.3***	0.1	2.6***	0.1	1.1***	0.0	0.8**	0.1	0.9**	0.1	0.4	0.0	66.8	4.7
Cr	43.0	3.0	44.0	10.1	41.7	7.6	41.3	2.4	47.7	3.4	48.6	2.7	62.0	6.5	41.6	4.1	93.4	22.7	63.4	5.4
Co	9.8	0.4	9.8	0.3	11.1	0.3	19.0***	0.1	21.8***	0.8	15.5	0.7	15.2	0.4	15.5	1.1	14.9	0.2	53.7	2.6
Cd	12.0***	1.4	12.6***	0.5	13.5***	0.9	20.0***	0.2	20.8***	0.9	3.2***	0.4	1.2***	0.0	0.8***	0.0	0.3	0.0	36.0	4.1
V	59.8	4.9	60.2	6.2	58.9	10.6	57.9	4.2	66.6	6.0	70.7	6.1	92.5	8.0	82.1	16.6	130.2	24.9	34.8	1.8
Ni	17.1	4.7	17.9	2.0	19.1	1.9	23.6	1.5	25.0	2.0	23.0	1.4	25.7	1.4	22.8	2.1	33.0	1.9	19.9	2.5
Mo	0.4	0.1	0.4	0.1	0.4	0.0	0.4	0.1	0.3	0.0	0.4	0.0	0.5	0.0	0.4	0.2	1.0	0.1	8.5	1.2
Sn	0.0	0.0	0.0	0.0	0.0	0.0	0.0	0.0	0.3	0.0	1.1	0.1	0.4	0.0	0.4	0.1	0.5	0.1	6.1	1.0
Se	0.0	0.0	0.0	0.0	0.0	0.0	0.0	0.0	0.0	0.0	0.0	0.0	0.0	0.0	0.0	0.0	0.2	0.2	5.3	0.5
Y	9.7	2.7	11.5	0.9	12.7	1.0	18.0	1.7	15.2	2.1	15.6	1.4	18.9	1.6	19.4	1.2	20.3	1.5	5.2	0.8
Th	6.2	0.4	7.2	0.7	6.6	0.7	6.8	0.6	8.3	0.9	7.9	0.5	9.2	0.2	8.2	0.6	9.6	0.5	3.7	0.1
In	6.5***	0.3	5.2***	0.2	3.0***	0.2	1.1**	0.2	0.1	0.0	0.1	0.1	0.1	0.0	0.1	0.0	0.1	0.0	2.9	0.1
Hg	0.5	0.2	0.3	0.1	0.2	0.1	0.2	0.1	0.1	0.0	0.1	0.0	0.3	0.1	0.2	0.0	0.4	0.1	2.6	1.0
Sc	7.0	0.5	7.6	1.5	7.5	1.4	7.2	0.5	7.0	0.2	7.6	0.5	8.3	1.4	7.9	0.9	17.6	5.0	2.2	0.3
U	1.6	0.3	2.2	0.6	3.3	0.3	4.0	0.3	1.6	0.1	1.5	0.2	1.9	0.2	1.6	0.3	1.5	0.3	2.2	0.3
Be	1.3	0.5	1.5	0.2	2.0	0.1	2.0	0.1	0.8	0.1	1.4	0.1	1.5	0.2	1.9	0.1	2.0	0.3	0.6	0.2
Au	0.1	0.0	0.1	0.1	0.2	0.0	0.1	0.0	0.0	0.0	0.1	0.0	0.2	0.1	0.3	0.1	0.2	0.1	0.2	0.1

* Significant at the 0.05 probability level.
** Significant at the 0.01 probability level.
*** Significant at the 0.001 probability level.

heavy metals and associated elements, with Zn and Cu presenting the highest concentrations. The Zn reached values of 23 090 mg kg^{-1}, this being 2.8-fold higher than in the tailings (Table 3) and 230-fold the content of uncontaminated soils (column UCS of Table 3). Meanwhile, Cu registered 11 480 mg kg^{-1} in the reddish-yellow layer—that is, 5.3-fold more than in the original tailings, and 446-fold greater than in nonpolluted soils.

The increase of the elements in the soils of the reddish-yellow layer can be ascribed to the secondary oxidation of the sulfides from the tailings (oxidative pollution), which, on changing to sulfates (Nordstrom, 1982), mobilized trace elements (Rogowski et al., 1977; Caruccio and Geidel, 1978), these in turn progressively penetrating the soil with the rainwater.

Depth Distribution of the Pollution

The distribution in depth of the 10 pollutant elements is presented in Fig. 5, showing that:

(i) The highest concentrations were consistently within the first 6 mm.
(ii) Substantial concentrations were invariably found in the upper 15 mm.
(iii) Below a certain depth (6 mm for As, Pb, Bi, Tl, Cu, and Sb; and 15 mm for Zn, Co, Cd, and In) the concentration in pollutant elements reached values similar to those of uncontaminated soils.
(iv) Nevertheless, Zn, Cu, Sb, Tl, and Cd showed small but significant accumulations at 100 to 150 mm.

Although all the elements dissolved in the acidic solution tended to accumulate in the first 15 mm of the soil, clear differences appeared. Thus Zn, Cu, Cd, and Co, the most mobile elements, showed similar distributions, with concentrations increasing from the upper zone (0–1 mm) downward, reaching the highest values near where the reddish-yellow layer met the underlying soil (4 mm). The Zn and Cu became less soluble where the soil pH was higher, reaching their highest precipitation values at pH 6.8 at 4 mm in depth. For the deepest zones, with pH values exceeding 7.6, concentrations fell drastically. The Cd and Co reached their highest accumulation at 4 to 6 mm, just below the reddish-yellow layer, and thus proved more mobile than Fe. The concentration in Co decreased to values lower than background in the uppermost part of the layer (0–3 mm), indicating that at pH < 6.4 this element dissolved and infiltrated the underlying soil (Fig. 5).

For As, Pb, In, Tl, Bi, and Sb, the concentrations declined intensely from the upper part (0–1 mm) downward, being less mobile than Fe. The Pb, As, and Bi did not reach the lower limit of the reddish-yellow layer, while the In and the Sb remained partially soluble at 15 mm in depth, with a pH of 7.9.

These results are consistent with previous observations. For example, Plant and Raiswell (1983) indicated that in oxidizing acidic environments, the relative mobility of Zn, Cd, Co, and Cu is considered high or moderately high, while that of Pb is low. Under neutral to basic conditions, relative mobility is considered low or very low for all of the elements.

Also, regarding the variations of heavy metals in depth, Martin and Bullock (1994) observed that in an acidic environment, Pb concentrations reached maximum values within the first centimeter, whereas Zn, Cd, and Cu reached higher values at 3 cm in depth. The concentrations of all of these metals diminished rapidly with depth, at 30 cm approaching background values.

With respect to the relative mobility of Fe, Simms et al. (2000) studied the distribution of total Zn and Fe, among other parameters, inside experimental columns filled with oxidized as well as unoxidized tailings, ob-

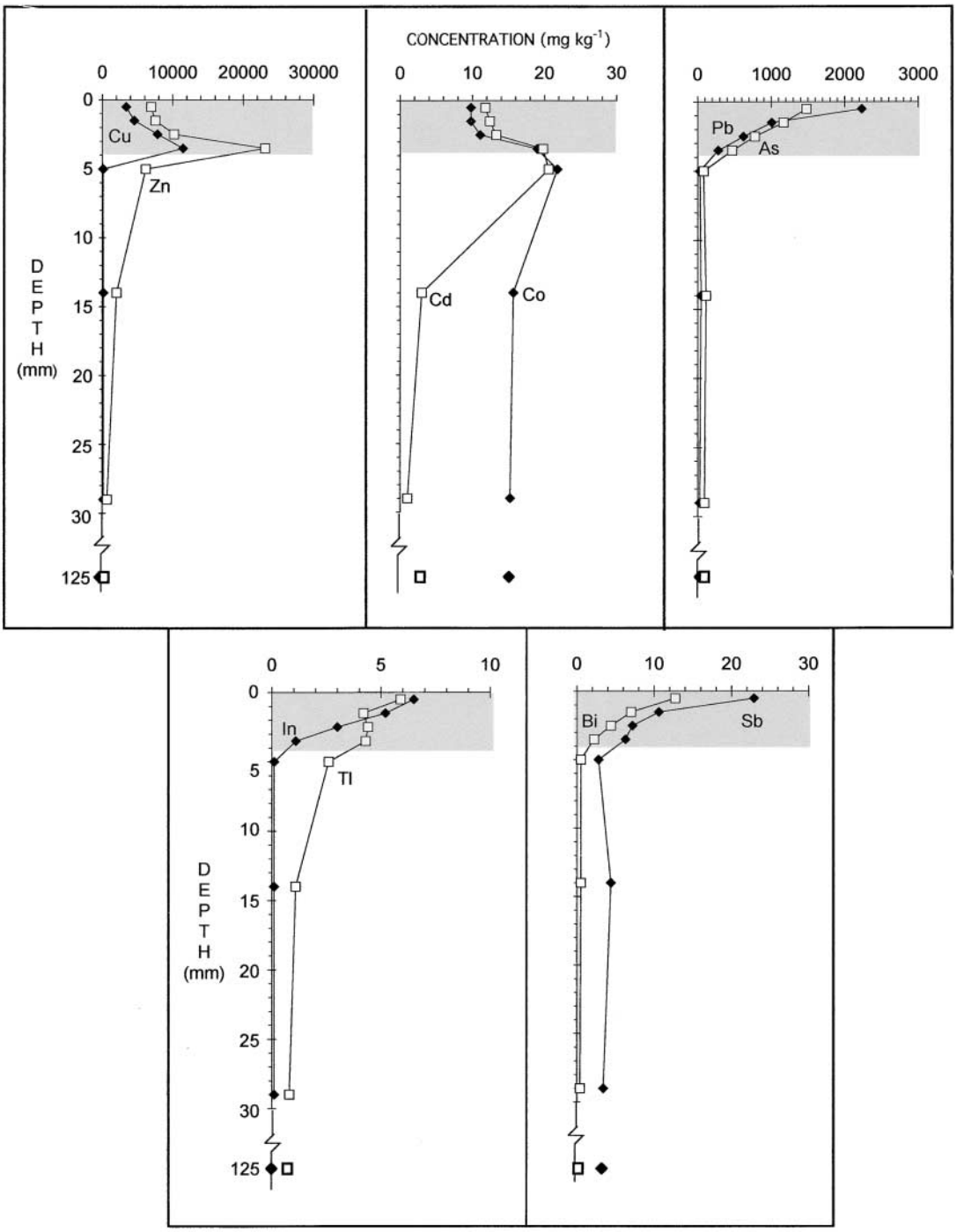

Fig. 5. Depth distribution (mean values) for the pollution of the different heavy metals and associated elements (in mg kg^{-1}). The grey zone represents the samples of the reddish-yellow layer.

serving that the highest Fe concentrations were reached at a shallower depth than were those of Zn. The pH of the oxidized zone was slightly lower than 6.0. In this sense, the mobility of Pb is less than of Fe in strongly acid media (Lindsay, 1981).

Migration Index

To evaluate the degree of mobility of the different pollutants, we calculated a migration index (MI) from the following equation, for the upper 0 to 30 mm (main zone of accumulation):

$$\mathrm{MI} = \sum_{n=1}^{7} (P/P_T)\, d$$

where n represents the layers sampled, P is the pollution of each element in each layer sampled, P_T is the sum of the pollution of each element of all layers sampled, and d the depth (mm) of the lower limit of each layer sampled. The value of this index would range from 1

(if the element accumulated entirely in the first 1 mm) to 30 (if the element accumulated entirely between 28 and 30 mm). The sequence of greater to lesser mobility would be (MI value in parentheses):

$$\text{Co (6.0)} > \text{Cd (4.3)} > \text{Zn (4.0)} > \text{Tl (3.6)} > \text{Sb (3.5)} > \text{Cu (3.2)} > \text{Pb (2.2)} > \text{In (1.9)} > \text{Bi (1.9)} > \text{As (1.8)}$$

For the same spill, comparable results were reported by Vidal et al. (1999) three months after the accident, with the exception of Tl, which these authors include among the elements of low mobility. This appears to indicate that Tl can decrease in mobility over time.

By ANOVA, we verified that all the MI values were highly significant ($p < 0.001$) and by Duncan test we divided the MI values into three subsets. Elements with high mobility were Co, Cd, and Zn; with moderate mobility, Tl, Sb, and Cu; and with low mobility, Pb, In, Bi, and As.

CONCLUSIONS

The infiltration into the soil of the acid solution formed by oxidation of pyrite tailings gave rise to weathering of the carbonates, acidification, and hydrolysis of the phyllosilicate particles (more intense the finer the particle size), but only in the first 4 mm of the soil. The SO_4^{2-} ions present in the acidic solution precipitated at this depth, forming gypsum, iron, and aluminum sulfates and complex sulfates. The Fe^{3+} ions also precipitated at this depth, apparently adsorbing a large part of the pollutants dissolved in the acidic solution. Most of these pollutants did not appreciably penetrate beyond 15 mm in depth, and large accumulations were found only in the first 6 mm.

For this type of toxic spill, our results indicate that in carbonate soils under a Mediterranean climate (and under study conditions), the pollutants tend to accumulate in the upper 0 to 15 mm of the soil, without contaminating the subsoil or ground water.

REFERENCES

Alastuey, A., A. García-Sánchez, F. López, and X. Querol. 1999. Evolution of pyrite mud weathering and mobility of heavy-metals in the Guadiamar valley after the Aznalcóllar spill, south-west Spain. Sci. Total Environ. 242:41–55.

Bertorino, G., A.M. Caredda, A. Ibba, and P. Zuddas. 1995. Weathering of Pb-Zn mine tailings in pH buffered environment. p. 859–862. *In* Y.K. Kharaka and O.V. Chudaev (ed.) Water–rock interaction. Proc. Symp., Vladivostok, Russia. 15–19 Aug. 1995. A.A. Balkema, Rotterdam, the Netherlands.

Cabrera, F., L. Clemente, E. Díaz Barrientos, R. López, and J.M. Murillo. 1999. Heavy metal pollution of soil affected by the Guadiamar toxic flood. Sci. Total Environ. 242:117–129.

Caruccio, F.T., and G. Geidel. 1978. Geochemical factors affecting coal mine drainage quality. p. 129–148. *In* F.W. Schaller and P. Sutton (ed.) Reclamation of drastically disturbed lands. ASA, CSSA, and SSSA, Madison, WI.

Eswaran, H., and S.A. Shoba. 1983. Scanning electron microscopy in soil research. p. 19–51. *In* P. Bullock and C.P. Murphy (ed.) Soil micromorphology. Vol. 1. Techniques and applications. AB Academic Publ., Berkhamsted, UK.

Förstner, U., and G.T.W. Wittmann. 1983. Metal pollution in the aquatic environment. Springer–Verlag, Berlin.

Johnson, D.W., and D.E. Todd. 1983. Relationships among iron, aluminium, carbon, and sulphate in a variety of forest soils. Soil Sci. Soc. Am. J. 50:776–783.

Kashir, M., and E.K. Yanful. 2000. Compatibility of slurry wall backfill soils with acid mine drainage. Adv. Environ. Res. 4:252–268.

Lindsay, W.L. 1981. Solid phase-solution equilibria in soils. p. 183–202. *In* R.H. Dowdy et al. (ed.) Chemistry in the soil environment. ASA Spec. Publ. 40. ASA and SSSA, Madison, WI.

Lopez-Pamo, E., D. Barettino, C. Antón-Pacheco, G. Ortiz, J.C. Arránz, J.C. Gumiel, B. Martinez-Pledel, M. Aparicio, and O. Montouto. 1999. The extent of the Aznalcóllar pyritic sludge spill and its effects on soils. Sci. Total Environ. 242:57–88.

Loveland, P.J., and W.R. Whalley. 1991. Particle size analysis. p. 271–328. *In* K.A. Smith and Ch.E. Mullis (ed.) Soil analysis: Physical methods. Marcel Dekker, New York.

Martin, M.H., and R.J. Bullock. 1994. The impact and fate of heavy metals in an oak woodland ecosystem. p. 327–365. *In* S.M. Ross (ed.) Toxic metals in soil–plant systems. John Wiley & Sons, West Sussex, UK.

Miedema, R., A.G. Jongmans, and S. Slager. 1974. Micromorphological observations on pyrite and its oxidation products in four Holocene alluvial soils in the Netherlands. p. 772–794. *In* G.K. Rutherford (ed.) Soil microscopy. Limestone Press, Kingston, ON, Canada.

Nordstrom, D.K. 1982. Aqueous pyrite oxidation and the consequent formation of secondary iron minerals. p. 37–56. *In* J.A. Kittrick et al. (ed.) Acid sulfate weathering. SSSA Spec. Publ. 10. SSSA, Madison, WI.

Nordstrom, D.K., and C.N. Alpers. 1999. Geochemistry of acid mine waters. p. 133–160. *In* G.S. Plumlee and M.J. Logsdon (ed.) The environmental geochemistry of mineral deposits. Part A. Processes, methods and health issues. Rev. Econ. Geol. 6A. Econ. Geol. Publ. Co., Littleton, CO.

Parfitt, R.L., and R.St.C. Smart. 1978. The mechanism of sulphate adsorption on iron oxides. Soil Sci. Soc. Am. J. 42:48–50.

Plant, J.A., and R. Raiswell. 1983. Principles of environmental geochemistry. p. 1–39. *In* I. Thornton (ed.) Applied environmental geochemistry. Academic Press, London.

Pons, L.J., N. Van Breemen, and P.M. Driessen. 1982. Physiography of coastal sediments and development of potential soil acidity. p. 1–18. *In* J.A. Kittrick (ed.) Acid sulfate weathering. SSSA Spec. Publ. 10. SSSA, Madison, WI.

Ritsema, C.J., and J.E. Groenenberg. 1993. Pyrite oxidation, carbonate weathering, and gypsum formation in a drained potential acid sulfate soil. Soil Sci. Soc. Am. J. 57:968–976.

Rogowski, A.S., H.B. Pionke, and J.G. Broyan. 1977. Modelling the impact of strip mining and reclamation processes on quality and quantity of water in mined areas: A review. J. Environ. Qual. 6:237–244.

Simms, P.H., E.K. Yanful, L. St-Arnaud, and B. Aubé. 2000. A laboratory evaluation of metal release and transport in flooded preoxidized mine tailings. Appl. Geochem. 15:1245–1263.

Simón, M., I. Ortiz, I. García, E. Fernández, J. Fernández, C. Dorronsoro, and J. Aguilar. 1999. Pollution of soils by the toxic spill of a pyrite mine (Aznalcóllar, Spain). Sci. Total Environ. 242:105–115.

Singer, P.C., and W. Stumm. 1968. Kinetics of the oxidation of ferrous iron. p. 12–34. *In* 2nd Symp. on Coal Mine Drainage Res., Pittsburgh, PA. 15–18 Oct. 1968. Bituminous Coal Res., Pittsburgh, PA.

Singh, B.R. 1984. Sulfate sorption by acid forest soils: 2. Sulfate adsorption isotherms with and without organic matter and oxides of aluminum and iron. Soil Sci. 138:294–297.

Stumm, W.Y., and J.J. Morgan. 1981. Aquatic chemistry: An introduction emphasizing chemical equilibria in natural waters. John Wiley & Sons, New York.

Van Breemen, N. 1973. Soil forming processes in acid sulfate soils. p. 66–130. *In* H. Dost (ed.) Acid sulfate soils. Proc. 1st Int. Symp., Wageningen, the Netherlands. 13–29 Aug. 1972. ILRI Publ. 18. Vol. 2. Int. Inst. for Land Reclamation and Improvement, Wageningen, the Netherlands.

Van Breemen, N. 1980. Magnesic-ferric iron replacement in smectite during aeration of pyritic sediments. Clay Miner. 15:101–110.

Vidal, M., J.F. López-Sánchez, J. Sastre, G. Jiménez, T. Dagnac, R. Rubio, and G. Rauret. 1999. Prediction of the impact of the Aznalcóllar toxic spill on the trace element contamination of agricultural soils. Sci. Total Environ. 242:131–148.

Wagner, D.P., D.S. Fanning, J.E. Foss, M.S. Patterson, and P.A. Snow. 1982. Morphological and mineralogical features related to sulphide oxidation under natural and disturbed land surfaces in Maryland. p. 109–125. *In* J.A. Kittrick et al. (ed.) Acid sulfate weathering. SSSA Spec. Publ. 10. SSSA, Madison, WI.

Williams, D.E. 1948. A rapid manometric method for the determination of carbonate in soils. Soil Sci. Soc. Am. Proc. 13:127–129.